Chandra reveals X-rays along the radio axis in the quasar 3C 9 at $z = 2.012$

A. C. Fabian,[1] A. Celotti[2]★ and R. M. Johnstone[1]

[1]*Institute of Astronomy, Madingley Road, Cambridge CB3 0HA*
[2]*SISSA, via Beirut, 2-4, 34014 Trieste, Italy*

ABSTRACT

A *Chandra* observation of the radio-loud quasar 3C 9 at redshift $z = 2.012$ has revealed extended X-ray emission coincident with the radio structure. Of particular interest is the appearance of X-ray emission on both sides of the nucleus, which argues against the X-ray emission being highly beamed. We present the properties and discuss possible scenarios for the X-ray emission, which is likely to be due to either non-thermal inverse Compton emission from relativistic electrons with small bulk Lorentz factor acting most probably on the cosmic microwave background but could involve infrared synchrotron photons or thermal emission from shocked cold gas surrounding the quasar. The thermal possibility implies a high mass for the cold gas unless it is highly clumped.

Key words: radiation mechanisms: non-thermal – galaxies: active – galaxies: jets – quasars: individual: 3C 9 – X-rays: galaxies.

1 INTRODUCTION

While the detection of X-ray emission coincident with radio jet structures is not unprecedented (e.g. Cen A, Schrieier et al. 1979; M87, Biretta, Stern & Harris 1991; 3C 273, Harris & Stern 1987; Röser et al. 2000), the *Chandra* X-ray Observatory (CXO) is providing an increasing quantity of high spatial and spectral resolution data on jetted structures associated with active galactic nuclei (AGN).

The first *Chandra* observation of a radio-loud quasar, PKS 0637–752, showed the presence of X-rays extending for ∼10 arcsec (Chartas et al. 2000; Schwartz et al. 2000). Furthermore, the X-rays have close spatial overlap with the known radio structure. Since then several jets observed with *Chandra* have shown associated X-ray emission (e.g. Pictor A, Wilson, Young & Shopbell 2001; Sambruna et al. 2002; Worrall, Birkinshaw & Hardcastle 2001; Pesce et al. 2001; Siemiginowska et al. 2002; Hardcastle et al. 2002a). It is important to stress that such features have been detected in both radio galaxies and blazars (i.e. objects observed at a small angle with respect to the inner jet direction). Furthermore *Chandra* allowed the detection of resolved X-ray emission from both hotspots and radio lobes (e.g. Brunetti et al. 2001; Hardcastle, Birkinshaw & Worrall 2001).

When multifrequency data are available (radio and optical images) interesting clues on the properties of the emitting plasma are obtained. In particular a rich phenomenology appears associated with jets, with different trends with distance from the core in different bands (an intensity decrease is often seen with X-rays whereas the radio often shows the opposite trend); displacements in the peak emission and different spatial extensions/components are sometimes visible in the images in different bands in the detailed comparison of individual knot emission. Broad-band information on spatially resolved structures has also been studied: the local broad band spectral energy distributions are often not straightforward to interpret, as in several cases the level of the X-ray emission is higher than simple models predict (e.g. Chartas et al. 2000; Schwartz et al. 2000; Röser et al. 2000; Harris & Krawczynski 2002). An analogous analysis can be performed on the multifrequency spectra of the lobes and hotspots.

Several radiation processes have been proposed to account for the emission of X-rays in jets (e.g. Celotti, Ghisellini & Chiaberge 2001), hotspots and lobes (e.g. Brunetti et al. 2001; Hardcastle et al. 2001). These include synchrotron radiation (possibly also from ultrarelativistic protons, Aharonian 2002) and inverse Compton scattering. The latter could be on seed photons of different origins, namely synchrotron, cosmic microwave background (CMB) and nuclear (hidden) blazar radiation. For jets, the most satisfactory model, involving inverse Compton scattering on the CMB (and likely synchrotron for the weakest sources), remarkably requires the presence of relativistic bulk flows on scale of ∼100 kpc. It also implies that the X-ray surface brightness of jets is constant with redshift, as pointed out by Schwartz (2002). Furthermore, structures in the jet velocity field, modelled as a relativistic core and a slower moving outer 'layer' (as already suggested on several other grounds), have been proposed to account for the varied phenomenology of both blazars and radio galaxies (e.g. Celotti et al. 2001). In the case of lobe emission, successful interpretation of the data can be obtained in some cases in the scenario where most of the emission originates

★E-mail: celotti@sissa.it

as inverse Compton on nuclear or CMB photons (Brunetti et al. 2001; Hardcastle et al. 2002b).

While much consensus on the above general scenario has accumulated, X-ray structures with looser morphological similarity to the radio jets have been found and proposed to be of thermal origin. In particular recent data from the radio galaxy PKS 1138-262 at $z = 2.2$ appear to support the view that a significant fraction of the detected X-ray flux arises from thermal, shock-heated, gas identified with the means for confinement for the radio-emitting plasma on large scales (Carilli et al. 2002).

The study of multifrequency emission from extended radio scales thus provides important information on the physics of jets and the interaction with their environment. Within this framework, we present here the discovery of large-scale X-ray emission associated with the quasar 3C 9, at $z = 2.012$, which has the highest radio luminosity in the 3CR catalogue. Most notably, the X-ray structure extends on both sides of the core, aligned with the radio structure. In this paper we present the data (Section 2) and discuss the possible origin of the emission (Section 3). Our brief conclusions are in Section 4.

2 OBSERVATIONS AND DATA ANALYSIS

3C 9 is a powerful quasar at redshift ~2 with extended radio emission (e.g. Bridle et al. 1994), classified as FR II. We observed it with *Chandra* for 16 235 s (cleaned of background flares) on 2001 June 10. 3C 9 was imaged on the back-illuminated ACIS-S3 chip. The data clearly show extensions to the north-west (NW) and south-east (SE) of the nuclear point source (Fig. 1). The X-ray structure corresponds well to that in the radio (Fig. 2), and in addition shows a 'spur' above the SE jet, and additional extended X-ray emission to the W of the nucleus.

Excluding the central region the counts in the SE and NW extensions are 18 and 12, respectively. While this of course does not allow any detailed spectral study, a simple power-law fit to the spectrum (grouped to a minimum of 10 counts per bin) gives a formal
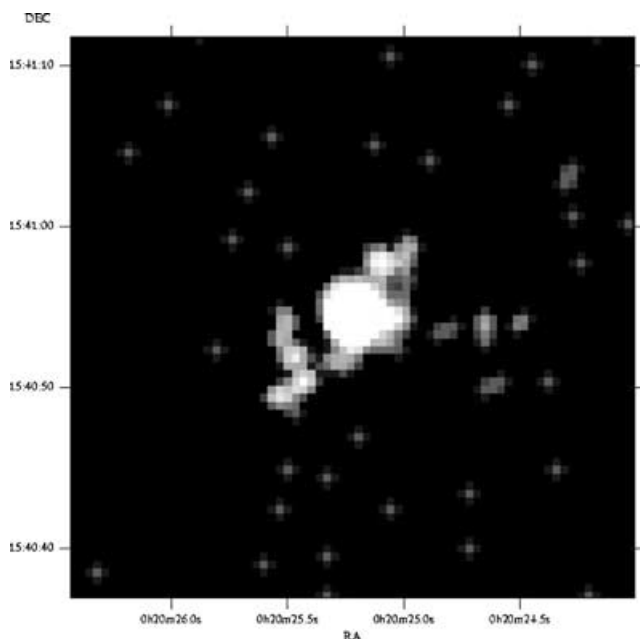
Figure 1. *Chandra* image of 3C 9 in the 0.5–5 keV band. Raw 0.5-arcsec pixels are used, smoothed by a Gaussian with standard deviation of 1 pixel.
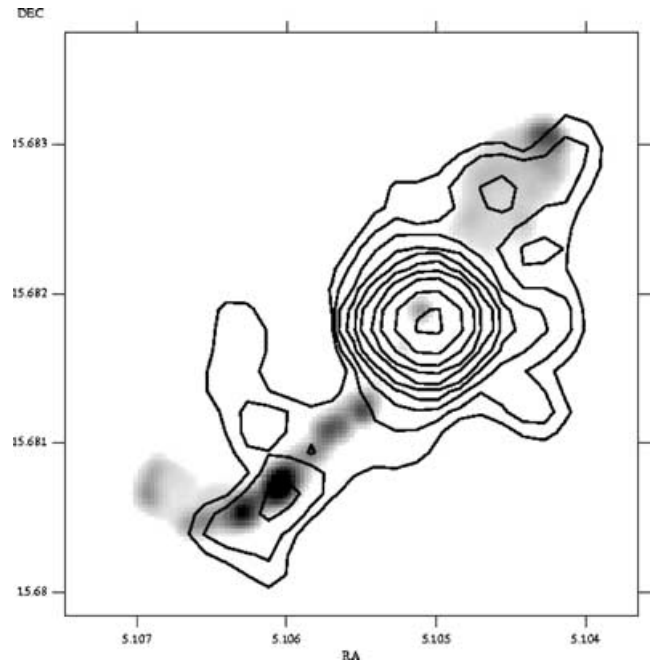
Figure 2. Overlay of 0.5–5 keV X-ray contours (after smoothing the original 0.5-arcsec binned image with a Gaussian that has a standard deviation of 0.5 arcsec) on the 4.9-GHz VLA radio map (from Bridle et al. 1994). The contours increase by factors of 1.9 from a level of 0.2 counts per 0.5-arcsec pixel. A possible ~0.5 arcsec offset between the images is within the pointing uncertainty of *Chandra*, and has not been corrected for.

spectral index $\Gamma_s = 1.6 \pm 0.6$ (with a normalization of $K = (2.8 \pm 0.9) \times 10^{-6}$ ph cm^{-2} s^{-1} keV^{-1} at 1 keV) assuming the Galactic value for $N_H = 4.2 \times 10^{20}$ cm^{-2} (Dickey & Lockman 1990). Uncertainties are quoted at the 90 per cent confidence level. The X-ray flux (0.4–5 keV) amounts to 1.23×10^{-14} erg cm^{-2} s^{-1} and the corresponding SE + NW extended luminosity is $\simeq 2.4 \times 10^{44}$ erg s^{-1} in the 2–10 keV band (rest frame) (assuming $H_0 = 50$ km s^{-1} Mpc^{-1} and $q_0 = 0.5$). A thermal (MEKAL) fit to the spectrum yields a minimum (quasar rest frame) temperature of 4.1 keV (at the 90 per cent confidence level) with no constraint on the upper temperature.

The nucleus suffers mild pile-up (at the 4 per cent level). Spectral fitting of a power-law continuum gives a photon index $\Gamma_s = 1.58 \pm 0.1$ (similar to that of the extended emission) and a flux of 1.45×10^{-13} erg cm^{-2} s^{-1} in the 0.2–3.5 keV band.

3 DISCUSSION

High-resolution Very Large Array (VLA) radio imaging of 3C 9 shows two knotty jets, lobes and hotspots (Bridle et al. 1994). As can be seen in Fig. 2, the comparison of the radio and X-ray images shows that the X-ray extensions roughly coincide with the overall radio features, although the SE structure does not extend beyond the jet bend observed in the radio.

The identification of the X-ray emission with specific radio components is difficult given the low count statistics. The brightest X-ray knots seem to be associated with the features A or B (NW hotspot or lobe) and H (SE knot) in the radio jet (the labels refer to those by Bridle et al. 1994, see their fig. 1). Nevertheless other features are visible, including the spur in the SE component, possibly associated with the analogous feature in the radio, and emission all

along the jets (both NW and SE). In order to determine the origin of the large-scale X-rays in 3C 9 we will therefore explore different possibilities for its spatial distribution and overall spectral energy distribution, assuming the observed X-rays are due to only one dominant process. Note that the poor constraints on the X-ray spectral index do not allow us to discriminate between non-thermal (steep synchrotron or flat inverse Compton) and thermal emission.

Let us start by considering that the X-ray emission is non-thermal radiation from the radio emitting electrons. As a reference, first compare the properties of 3C 9 with those of PKS 0637–752, at $z = 0.654$. The total low-frequency radio fluxes (at 408 MHz) of the two systems are similar, whereas the extended X-ray flux is a factor ~ 10 lower in 3C 9 (Schwartz et al. 2000). Also the nuclear (blazar-like) X-ray emission of PKS 0637–752 exceeds that of 3C 9 by a similar factor (~ 10–50, Wilkes et al. 1994). This implies that both the X-ray extended jet emission and (especially) the blazar core in 3C 9 are less prominent, with respect to the presumably isotropic extended radio emission, than in PKS 0637–752. The differing prominence of the blazar component could be simply ascribed to a difference in the angle between the (core) jet and the line of sight, as envisaged by unification schemes. This is indeed supported by the flat ($\alpha_R \sim 0$) radio spectrum of PKS 0637–752 (between 408 MHz – 4.85 GHz; Wright et al. 1994; Large et al. 1981) and also by the detected superluminal motion which indicates bulk Lorentz factors (relative to the core jet) $\Gamma_b > 17$ and an angle between the jet axis and line of sight $\theta < 6$ deg (Lovell et al. 2000). On the other hand, a steep ($\alpha_R \sim 1$) spectrum dominates the radio emission in 3C 9 (between 1.4–14.9 GHz to compare a similar intrinsic spectral range; Laing & Peacock 1980; White & Becker 1992).

What can we then infer about the dominant radiation mechanism for the extended X-ray emission in 3C 9?

3.1 Non-thermal synchrotron emission

First of all, a comparison of the radio to X-ray luminosity, whether from the jet knots, hotspots or lobes, shows that the X-ray power exceeds the radio power by about a factor of 5. In order for the X-rays to have a synchrotron origin, therefore, the spectrum should flatten above the radio range to a value $\alpha \sim 0.8$–0.9. Note that, by assuming equipartition, Bridle et al. (1994) infer typical values of the magnetic field of order $B_{eq} \sim (1 - 7) \times 10^{-4}$ G, corresponding to an energy density $u_{B,eq} \sim (0.04 - 2) \times 10^{-8}$ erg cm^{-3}. We note that, with such magnetic fields, the estimated cooling time-scales (for electrons emitting at ~ 10 GHz) would only amount to 10^4 yr all along the radio structure, despite the extent of the lobes, possibly suggesting that at least in some regions B_{eq} might be an overestimate of the actual field. In any case the corresponding lifetime for electrons emitting via synchrotron in the X-rays would be unrealistically low ($\sim$yr) for such an extended structure arguing against a synchrotron origin of the X-rays (in situ particle re-acceleration would in fact have to occur distributed and continuous in most of the entire jet volume), unless the average field is orders of magnitude smaller than the equipartition value.

3.2 Non-thermal inverse Compton emission

A likely alternative to synchrotron emission is that the X-rays are produced as inverse Compton radiation. Let us then consider the possible sources of soft photons and compare the corresponding radiation energy densities. The radiation field in the CMB is of order $u_{CMB} \sim 3 \times 10^{-11}$ erg cm^{-3}, and if seen by relativistically moving

plasma (as in e.g. PKS 0627–752) it can exceed this value by a couple of orders of magnitude. Note also that if the X-ray emission is not beamed the electrons responsible for the X-ray and radio emission have comparable energy, implying – for an equipartition magnetic field – a similarly short lifetime (see above), again arguing for a sub-equipartition field.

The CMB radiation field appears to dominate over the possible radiation from the nucleus, $u_{nuc} \sim 3 \times 10^{-12} L_{47} R_{100\,kpc}^{-2}$ erg cm^{-3}, if the luminosity in the (synchrotron) blazar component is of order $L \sim 10^{47} L_{47}$ erg s^{-1} and $L_{47} \sim 1$. A scattered nuclear origin of the seed photons would thus require blazar (synchrotron) emission with at least $L_{syn} \sim 10^{48-49}$ erg s^{-1} (as 'seen' by the radio source) making it one of the brighter (if not the brightest) known blazars and require a high value of the Lorentz factor. Although this might appear unlikely we note that 3C 9 is one of the highest redshift and most radio luminous object in the 3CR catalogue.

The energy density in target synchrotron photons for the Synchrotron Self-Compton (SSC) process accounts for $u_{syn} \sim 4 \times 10^{-13}$ erg cm^{-3}, if only the observed radio luminosity is considered. In fact the synchrotron luminosity might be significantly underestimated if the spectrum extends above the radio range with a slope flatter than ~ 1, possibly dominating the total energy output (consistently with the very high equipartition field). In particular, in order to compete with the (unbeamed) CMB photon field, the spectrum should extend from the radio to typically the optical range with a slope flatter than $\alpha \sim 0.5$. The corresponding flux $\gtrsim 10^{-13}$ erg cm^{-2} s^{-1} should be detectable by the *Hubble Space Telescope* (*HST*), but it is not evident on an archival snapshot, suggesting that the peak of the synchrotron component would have to be at infrared energies (with a flatter radio–infrared spectrum). Finally note that the origin of X-rays as scattered nuclear or synchrotron photons is also supported by the morphology of the emission, as in 3C 9 the X-ray structures extend (within the limits of resolution) over the entire radio structure, while e.g. in PKS 0637–752 it appears one sided and strongly peaks in the large distance knots, at several hundred kpc from the nucleus.

Although the uncertainties in the above estimates do not allow us to identify uniquely the most likely seed field, we can consider another piece of information, namely the ratio of the fluxes in the SE and NW components, both in the radio and X-ray bands. In the radio such a ratio strongly depends on the considered components. The inner (straight) part of the jets – possibly a good indicator of the jet speed and orientation near its base – is consistent with ~ 3.3, implying small values of Γ_b even for an angle of $80°$ (note that unification models would suggest $45°$ as an indicative limit for a quasar), suggesting that the nucleus and inner jet of 3C 9 are observed at large viewing angle (consistent with the above considerations from the comparison with PKS 0637–752). However on larger scales the jets appear to become more asymmetric, both in extension and in brightness: the ratio of the total jet versus counter-jet emission amounts to ~ 900 (Bridle et al. 1994), possibly indicating that the jets bend between the small and large scales (see also Bridle et al. 1994) and even that we might thus be looking at some relativistically beamed emission. A small ratio (~ 0.3) characterizes the emission from the hotspots. We note however that no X-ray emission appears to originate in the SE hotspot (after the jet bend) excluding the hotspot origin as a unique source of X-rays and suggesting that at the jet bend either the speed of the jet decreases, the angle to the line of sight increases and/or the relativistic electrons do not intercept anymore the nuclear beamed radiation. These results therefore do not allow us to discriminate among the above emission models.

However, a further piece of information is the ratio of the flux in the SE and NW components in the X-ray band. As this is in the range 0.9–2.6 the X-ray emission is not highly beamed. The high energy radiation can then originate in a slowly moving (layer?) component of the jet or in the lobes. Note that this flux ratio is also compatible with the effect of anisotropic scattering of the nuclear light (as estimated by Brunetti et al. 2001) for relatively large jet angles.

3.3 Thermal emission

While the evidence discussed so far might be reasonably (although not uniquely) convincing, an alternative view could ascribe the majority of the X-ray flux to thermal emission, as suggested by Carilli et al. (2002), from gas heated via shocks produced by the jet propagation and able to confine the jet itself. Indeed the quality of the morphological similarity between the radio and X-ray spatial distribution – even the evidence of a (spatially coincident) knot (in the SE extension) – cannot distinguish between these possibilities. As already noted the spectral analysis cannot constrain the nature of the emission and the SE/NW extension ratio is consistent (due to the paucity of counts) with a similar, isotropic emission from the two sides.

An additional constraint on X-ray emission models is the extended Lyman α nebula around 3C 9 found by Heckman et al. (1991), with a tentative detection in Lyman α of a structure coincident with brighter part of the SE jet. This means that there is extensive ionized gas around the quasar, possibly at high gas pressure, as inferred by the redshifted Hα and [O III] observations reported by Wilman, Johnstone & Crawford (2000). If the extended X-ray emission is thermal bremsstrahlung then, assuming an emission temperature of 10 keV for the shocked gas and an approximate volume of $10 \times 10 \times 50$ kpc^3, the electron density is about 0.5 cm^{-3} meaning a pre-shock density of ~ 0.1 cm^{-3}. This is high if the pre-shock temperature is 1 keV or more, comparable only to that seen in the centres of strong cooling flows in nearby rich clusters. The pressure of the shocked gas is comparable to that deduced from oxygen line ratios by Wilman et al. (2000) for gas at about 13 kpc from the nucleus which gives some support to this possibility. However clouds around powerful low redshift radio galaxies appear to be overpressured (Robinson, Tadhunter & Dyson 2002), and the *Chandra* data are inconsistent with the extensive intracluster medium of a rich cluster around the quasar. (Ignoring the weak temperature dependence, the emissivity of the pre-shock gas is 1/16 of that post-shock, so a volume 16 times that of the jet should have a similar flux which for a cylinder corresponds to a radius of about 4 arcsec; the data at this radius are however entirely consistent with the background.) The shock velocity must exceed about 2000 km s^{-1} to agree with our lower limit on the gas temperature. The total mass of shocked gas (assuming unit filling factor f of the volume assumed above) is about 10^{11} M$_\odot$. Presumably there is much more gas beyond the region now shocked which occupies only a few per cent of the volume within the radius of the jet, raising the total gas mass to above 10^{12}M$_\odot$. The mass varies as $f^{1/2}$, requiring a very low filling factor (say, $f \sim 10^{-3}$) if the mass is to be significantly reduced.

Only if the gas is cooler can high pre-shock densities be present and consistent with observations. The difficulty is then accounting for such an extensive and massive atmosphere of relatively dense gas. It might have to be in the form of many small dense cold clouds in order to minimize the mass. Perhaps both the X-ray and Lyman

α emissions are due to shocks and photoionization of a substantial mass of cold gas clouds which are remnants of galaxy formations and mergers.

4 CONCLUSIONS

In summary, there are difficulties with all plausible models, largely due to a lack of good infrared-optical to X-ray data. The simplest explanation is that we are seeing unbeamed inverse Compton X-ray emission from relativistic electrons acting on the CMB. In this case the field must be below equipartition. Alternatively, it can be SSC, which however requires significant synchrotron emission in the infrared band, or clumpy thermal emission.

Clearly, it is of great relevance to distinguish between these scenarios with higher quality data, which will allow the non-thermal plasma and thermal shocked gas possibilities to be distinguished, thereby constraining either the jet velocity field, dissipation and particle acceleration processes, or the interaction of the jet structure with its confining medium.

REFERENCES

Aharonian F., 2002, MNRAS, 332, 215
Biretta J. A., Stern C. P., Harris D. E., 1991, AJ, 101, 1632
Bridle A. H., Hough D. H., Lonsdale C. J., Burns J. O., Laing R. A., 1994, AJ, 108, 766
Brunetti G., Cappi M., Setti G., Feretti L., Harris D. E., 2001, A&A, 372, 755
Carilli C. L., Harris D. E., Pentsrissi L., Röttgering H. J. A., Mily G. K., Kurk J. D., van Breugel W., 2002, ApJ, 567, 781
Celotti A., Ghisellini G., Chiaberge M., 2001, MNRAS, 321, L1
Chartas G. et al., 2000, ApJ, 542, 655
Dickey J. M., Lockman F. J., 1990, ARA&A, 28, 215
Hardcastle M. J., Birkinshaw M., Worrall D. M., 2001, MNRAS, 323, L17
Hardcastle M. J., Worrall D. M., Birkinshaw M., Laing R. A., Bridle A. H., 2002a, MNRAS, 334, 1821
Hardcastle M. J., Birkinshaw M., Cameron R. A., Harris D. E., Looney L. W., Worrall D. M., 2002b, ApJ, in press
Harris D. E., Krawczynski H., 2002, ApJ, 565, 244
Harris D. E., Stern C. P., 1987, ApJ, 313, 136
Heckman T. M., Lehnert M. D., Van Breugel W., Miley G. K., 1991, ApJ, 370, 78
Laing R. A., Peacock J. A., 1980, MNRAS, 190, 903
Large M. I., Mills B. Y., Little A. G., Crawford D. F., Sutton J. M., 1981, MNRAS, 194, 693
Lovell J. E. S. et al., 2000, in Hirobagashi H., Edwards P. G., Murphy D. M., eds, Astrophysical Phenomena Revealed By Space VLBI. ISAS, Sagamihara, p. 215
Pesce J. E., Sambruna R. M., Tavecchio F., Maraschi L., Cheung C. C., Urry C. M., Scarpa R., 2001, ApJ, 556, L79
Robinson T. G., Tadhunter C. N., Dyson J. E., 2002, MNRAS, 331, L13
Röser H.-J., Meisenheimer K., Neumann M., Conway R. G., Perley R. A., 2000, A&A, 360, 99
Sambruna R. M., Maraschi L., Tavecchi F., Urry C. M., Cheung C. C., Chartas G., Scarpa R., Gambil J. K., 2002, ApJ, 571, 206
Schieier E. J., Feigelson E., Delvaille J., Giacconi R., Grindlay J., Schwartz D. A., Fabian A. C., 1979, ApJ, 234, L39

Schwartz D. A. et al., 2000, ApJ, 540, L69
Schwartz D. A., 2002, in Gilfanov M., Sunyaev R., Churazov E., eds, Proc. ESO Astrophys. Symp. Lighthouses of the Universe. Springer-Verlag, Berlin, p. 538
Siemiginowska A., Bechtold J., Aldcroft T. L., Elvis M., Harris D. E., Dobrzycki A., 2002, ApJ, 570, 543
White R. L., Becker R. H., 1992, ApJS, 79, 331

Wilman R. J., Johnstone R. M., Crawford C. S., 2000, MNRAS, 317, 9
Wilson A. S., Young A. J., Shopbell P. L., 2001, ApJ, 547, 740
Worrall D. M., Birkinshaw M., Hardcastle M. J., 2001, MNRAS, 326, L7
Wright A. E., Griffith M. R., Burke B. F., Ekers R. D., 1994, ApJS, 91, 111

This paper has been typeset from a TEX/LATEX file prepared by the author.